INTERNATIONAL JOURNAL OF HYDROGEN ENERGY XXX (2017) 1–18

Available online at www.sciencedirect.com

ScienceDirect

journal homepage: www.elsevier.com/locate/he

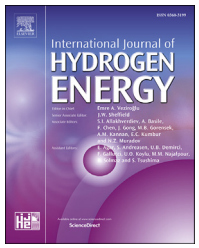

Tri-generation for industrial applications: Development of a simulation model for a gasification-SOFC based system

Valeria Palomba [a,b,*], *Mauro Prestipino* [a], *Antonio Galvagno* [a]

[a] *University of Messina, Department of Engineering, C.da Di Dio (Vill.S.Agata), Messina, 98166, Italy*
[b] *National Council of Research, Institute for Advanced Energy Technologies ITAE, Via Salita Santa Lucia Sopra Contesse 5, Messina, 98126, Italy*

ARTICLE INFO

Article history:
Received 27 February 2017
Received in revised form
23 June 2017
Accepted 26 June 2017
Available online xxx

Keywords:
Gasification
SOFC
Trigeneration
Simulation
Energy analysis

ABSTRACT

Combined Cooling, Heat and Power production (CCHP) systems allow energy production with high efficiencies. An even higher advantage can be obtained by feeding the system with biomass or residues. In the present paper, the development of a simulation model of a CCHP system of 630 kW_e size is presented. An ASPEN model has been developed for the simulation of a gasification-SOFC plant with a downdraft gasification process from lignocellulosic biomass. The results of the model have been used to set a model of the whole CCHP system in TRNSYS environment, suitable for dynamic simulations. The model has been applied to an industrial case study, which represents an advancement of the current literature, and different layouts have been evaluated. Such models include not only standard components, such as vapour compression chillers but also advanced thermal chillers. Results showed that the primary energy consumption using a CCHP system could be reduced of about 15 GWh/y (50% less of a traditional system with separate energy production) with an amount of avoided CO_2 emissions of about 5000 t/y.

Introduction

CO_2 emissions are a key issue in today's global energy scenario, due to an increasing commitment towards the environment and the containment of climate change [1]. Among the factors contributing to the increasing amount of GHG in atmosphere, industrial activities cover a primary role. In particular, burning of fossil fuels is the primary source of GHG emissions [2]. To overcome or mitigate such an issue, the utilization of alternative energy sources, e.g. green renewable fuels, can be beneficial [3,4]. Indeed, biomasses are a renewable and carbon neutral resource, which is widely available worldwide. Lignocellulosic biomass, such as wood, have been traditionally processed by combustion for power production, even if pyrolysis and gasification can be also used for producing power and/or fuels efficiently, using different types of feedstocks [5–9]. Among the different technologies of lignocellulosic biomass conversion for power production, thermochemical gasification allows high efficiency and lower pollutant emission per unit power, in particular in small-scale applications [5]. Indeed, syngas can efficiently take advantages by the well-established technologies of internal combustion engines or gas turbines [10–13].

* *Corresponding author*. National Council of Research, Institute for Advanced Energy Technologies ITAE, Via Salita Santa Lucia Sopra Contesse 5, Messina, 98126, Italy.
E-mail address: valeria.palomba@itae.cnr.it (V. Palomba).

http://dx.doi.org/10.1016/j.ijhydene.2017.06.206
0360-3199/

Nomenclature

A	area, m^2
c_p	specific heat capacity, kJ/(kgK)
E	energy, MWh
F	Faraday constant, C/mol
G	solar radiation, W/m^2
I	current, A
$\dot{m}$	mass flow rate, kg/h
n	molar flow, kmol/h
P	electric power, kW
PE	Primary energy, MWh
$\dot{Q}$	thermal power, kW
T	temperature, °C
U	overall heat transfer coefficient, $W/(m^2K)$
V	voltage, V
V_N	Nernst voltage, V
x	molar fraction of gaseous components

Greek letters

η	efficiency

Subscripts

a	activation
amb	ambient
aux	auxiliaries
biom	biomass
c	concentration
cg	cold gas
CL	cooling load
comb	combustion
comp	compressors
elec	electric
EL	electric load
ex	excess
HL	heating load
in	inlet
m	average temperature
NRES	Non Renewable Energy System
pd	production and dispatch
out	outlet
RES	Renewable Energy System
syn	syngas

Abbreviations

AC	Alternating Current
CHP	Combined Heat and Power
CCHP	Combined Cooling Heat and Power
COP	Coefficient of Performance
DC	Direct Current
EER	Energy Efficiency Ratio
GHG	GreenHouse Gases
KPI	Key Performance Indicator
HT	High Temperature
LHV	Low Heating Value, MJ/Nm3
LT	Low Temperature
MT	Medium Temperature
SOFC	Solid Oxide Fuel Cell
VCC	Vapour Compression Chiller

Combined heat and power (CHP) systems allow producing both thermal and electrical energy with high efficiencies [14–17]. If CHP systems are combined with the use of by-products, biomass or residues, additional environmental and economic benefits may be achieved. Among the technologies available for CHP, high temperature fuel cells, such as molten carbonate and solid oxide fuel cells, can operate on carbon-based fuels derived from biomasses or by products with high efficiencies [18–21], high reliability and low NOx and SOx emissions [22]. A further beneficial effect of using SOFC systems for power production is the possibility to recover and reuse the produced CO_2, as suggested by Santarelli et al. [23].

The biomass-fuelled configuration for SOFC has been proposed by many authors [24–27], which show the potential of such solutions by achieving net electrical and CHP efficiencies in the range of 32–47% and 74–80%, respectively [27,28].

The application of SOFCs in trigeneration (CCHP) or polygeneration system leads to other advantages, since it is possible to reutilize all or part of the heat from SOFC for cooling production, further increasing the overall efficiency of the plant. An extensive review of the technology of fuel cells applied to CCHP is reported in Ref. [29]. In literature, several studies are cover the topic of the coupling of SOFC and thermally driven systems for CCHP production. In Ref. [30], Calise presents the design and economic analysis of a polygeneration system for CCHP production, using a concentrated solar field, a SOFC and an absorption chiller. A MATLAB model is used for the simulation of the fuel cell, while TRNSYS environment is used for the design of the integrated system. In Ref. [31], the TRNSYS simulation of a CCHP system including evacuated solar collectors, a PEM fuel cell and an absorption chiller is reported and overall energy consumption and economic figures are calculated for an office building (i.e. a portion of university building). However, most of the studies reported in literature, while dealing with TRNSYS models in different climates, are almost solely focused on the residential sector for heating [32,33], cooling [34], heating and cooling [35] or heating cooling and domestic hot water production [26].

In such a context, aim of the present study is to present the analysis of different solutions for the application of a SOFC-based trigeneration system in an industrial background, for the production of process heating, cooling and electricity. A wood processing industry was selected for developing the analysis of this case study. The SOFC fed by syngas, obtained from the gasification of lignocellulosic biomass, is used for heating and electricity production. The gasification unit was fed by the pinewood residues produced during wood processing of the considered industry. Instead, cooling demand is met by either an adsorption chiller or a vapour compression chiller. Moreover, in addition to the SOFC, the use of solar collectors for heating supply has been evaluated, which represents a novel analysis for the secondary sector. To this goal, two models were realised: an ASPEN Plus model for the simulation of the biomass gasification and SOFC units and a TRNSYS model for the integration of the SOFC into the whole trigeneration system. All the models are based on validated components. Results are reported in terms of primary energy saved for the system, as well as the reduction in CO_2 emissions, in comparison to the standard Italian energy mix. The

Please cite this article in press as: Palomba V, et al., Tri-generation for industrial applications: Development of a simulation model for a gasification-SOFC based system, International Journal of Hydrogen Energy (2017), http://dx.doi.org/10.1016/j.ijhydene.2017.06.206

global system efficiency of each solution has been calculated and the results compared.

The case study

Heating, cooling, electric loads

Focus of the present study is the application of a solid oxide fuel cell unit, fed by syngas from biomass, to the case of an industrial application. With respect to the residential cases analysed in literature, the industrial needs differ not only in the sizing of the whole system, but also in the characteristics of the load itself. Whereas the cooling and heating profile of a building are mostly influenced by external weather conditions [26,33,35], the demand for the industry is mainly due to the process heating or cooling requests and is therefore more stable. This is an advantage when dealing with CHP and CCHP systems, for which a higher capital cost is needed and difficult in following the thermal profile is, in some cases, found [36]. For the analysis, the actual electricity, heating and cooling demand of an Italian wood processing industry have been used for the simulation. Such contributes are shown in Fig. 1 on monthly basis. As clearly shown, in this case, the cooling demand is constant and it is only a fraction (around 20%) of the heating energy needed. Instead, the electric load contributes to about a third of the total request of the system. Since the hourly profile for the loads are known, the power needed has been calculated as well, in order to size the SOFC-powered system. Even though a SOFC could be able to follow quick load change, this could also imply possible damages [25]. It follows that the criterion used for sizing the SOFC was to cover the electrical power base-load demand (Fig. 1) at every condition, considering the possibility to sell any produced electricity surplus. From the calculated values, a fuel cell system of 630 kW_{el} net electrical power has been considered. Two working points have been selected: 630 kW_{el} from May to November and 540 kW_{el} from January to April and in December. The system operates for 8040 h/y, since in August and December the industry stops for 15 days for periodic maintenance.

System layout

The actual power generation system (named "reference system") installed in the industrial site, relies mostly on energy from fossil fuels: the electricity is completely obtained by the connection to the national grid, whereas, for the satisfaction of cooling loads, electrically-operated vapour compression chillers (VCC) are used. Regarding the heating loads, these have been further divided into hot water demand (at 80 °C) and steam demand (at 175 °C and 8 bar g). In the reference system, they are all covered by methane boilers.

Since the aim of the work here presented is the evaluation of different alternatives, three layouts have been compared, which differ in the number and type of energy sources and the destination of heat and electricity produced by the SOFC. A summary of the simulated cases is reported in Table 1, where the source used to satisfy each energy demand contribute is described. For comparison reasons, the reference system is described.

In Fig. 2, the schematic layout for each of the three cases is reported.

In each system, there are a gasificator and a SOFC system, representing the core of the whole power generation architecture. The gasification unit that has been considered in this work is a fixed bed downdraft reactor. The SOFC represents the syngas utilization section, i.e. the power generation unit, which is modelled by a tubular solid oxide fuel cell developed by Siemens Power Generation Inc. This type of solid oxide fuel cell has been proven to be reliable, working over 36,000 h fed by natural gas [25] and it is easy to scale [37]. The SOFC system examined in this work consisted in the combination of seven 120 kW DC stacks, for a total gross DC electrical output of 840 kW.

In case 1, an adsorption chiller is used to meet cooling loads. For the simulation, a silica-gel/water commercial

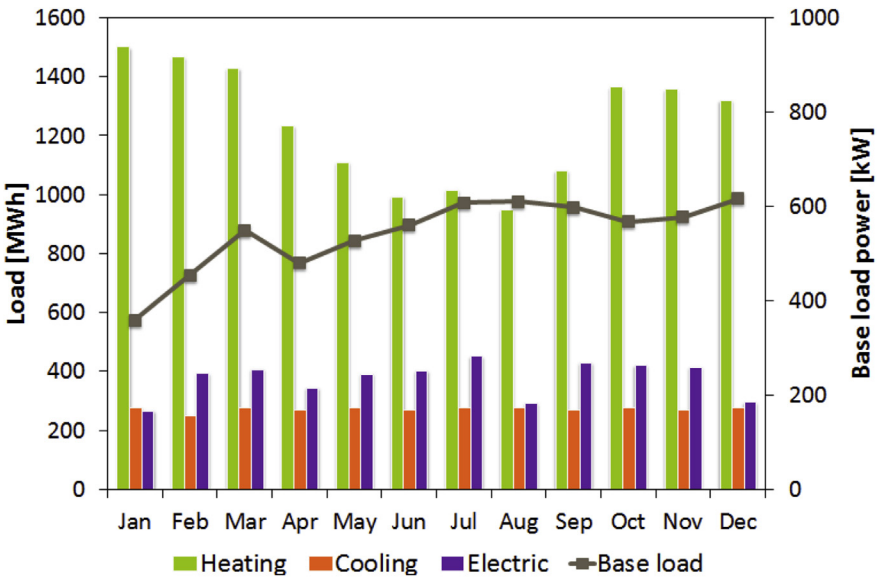

Fig. 1 – Annual load demand for the examined case.

Please cite this article in press as: Palomba V, et al., Tri-generation for industrial applications: Development of a simulation model for a gasification-SOFC based system, International Journal of Hydrogen Energy (2017), http://dx.doi.org/10.1016/j.ijhydene.2017.06.206

Table 1 – The scenarios modelled.

		Case 1	Case 2	Case 3	Reference
Electric		SOFC	SOFC	SOFC	National electric grid
	Back- up	National electric grid	National electric grid	National electric grid	–
Heating		SOFC	SOFC	SOFC + evacuated solar collectors	Methane boilers
	Back- up	boiler	boiler	boiler	–
Cooling		Adsorption chiller driven by waste heat from SOFC	Compression chiller driven by electric energy from SOFC	Compression chiller driven by electric energy from SOFC	Compression chiller driven from national electric grid
	Back- up	No	National electric grid	National electric grid	–

adsorption unit, whose performance have been experimentally measured at CNR-ITAE laboratories, has been used as basis. For the rejection of process heat, the chiller is equipped with a dry re-cooling system using variable speed fans. The adsorption chiller is driven through the hot water produced by the SOFC system. Indeed, in order to guarantee an almost constant inlet to the adsorption chiller, and allow for the utilization of the heat from the fuel cell also for heating purposes, a sensible heat hot water storage has been inserted. It is connected to the fuel cell and a back-up heater.

For cases 2 and 3, a vapour compression chiller with R410a gas as refrigerant has been considered. As for the case of the adsorption chiller, the condensation heat is rejected through a variable speed fans dry re-cooler. In both these cases, a sensible heat hot water storage has been inserted:

- In case 2, it is connected to a heat exchanger recovering the heat from the SOFC and the methane boiler. It serves for the coverage of the heating loads.
- In case 3, the storage is heated by a solar field made up of evacuated tube collectors and the fuel cell, while no boiler serves as back-up. As for the previous case, all the heat is used to follow the "hot water" loads.

In all the cases studied, the existing diathermic oil boiler (operated by methane) has been maintained for the production of steam.

For case 3, a solar field has been considered, made up of evacuated tube collectors. Indeed, they guarantee, with respect to other types of solar collectors, a higher efficiency and a temperature level (75–90 °C) suitable to drive the adsorption chiller [38]. The solar collector field has been designed in order to cover the fraction of thermal heating load that, according to its nominal characteristics, the fuel cell could not satisfy.

Methodology

In Fig. 3, the methodology followed for the analysis is represented. As stated before, the main aim of the study is the evaluation of benefits arising from the use of the CCHP system over the traditional one, in terms of primary energy savings and reduction of GHG emissions (specifically CO_2). In order to ensure the reliability of the models, validation studies have been performed, on both the gasification/fuel cell section and the solar/adsorption one.

From the gasification-SOFC model, the efficiencies of this system has been calculated in order to verify the impact of this solution on the existing plant and to find the critical points for the improvement of the system. Different efficiency parameters have been calculated: cold gas efficiency, SOFC gross and net electrical efficiency and CHP gross and net efficiency. Cold gas efficiency (η_{cg}) defines the efficiency of intrinsic chemical energy conversion of biomass into syngas, expressed as follows:

$$\eta_{cg} = \frac{\dot{m}_{syn}\, LHV_{syn}}{\dot{m}_{biom}\, LHV_{biom}} \tag{1}$$

where $\dot{m}_{syn}$ and $\dot{m}_{biom}$ are the syngas and biomass mass flows, respectively, LHV_{syn} is the syngas low heating value and LHV_{biom} is the biomass low heating value.

The SOFC gross electrical efficiency ($\eta_{SOFC,gross}$) is the ratio between the SOFC AC electrical output ($P_{AC\ gross}$) and the syngas power input ($\dot{m}_{syn} \cdot LHV_{syn}$), while the net electrical efficiency ($\eta_{SOFC,net}$) also consider the compressors power consumptions (P_{comp}).

Moreover, the gross AC efficiency and the CHP efficiency ($\eta_{CHP,\ gross}$) of the gasification-SOFC section have been calculated. The former is the ratio between the gross electric output ($P_{AC\ gross}$) and the total fuel power input ($\dot{m}_{biom}\, LHV_{biom}$), while the latter is the sum of the gross electric output and useful thermal output ($\dot{Q}_{SOFC}$) produced by the fuel cell, divided by the energy input from the fuel.

$$\eta_{SOFC,\ gross} = \frac{P_{ACgross}}{\dot{m}_{syn} \cdot LHV_{syn}} \tag{2}$$

$$\eta_{SOFC,net} = \frac{P_{ACgross} - P_{comp}}{\dot{m}_{syn} \cdot LHV_{syn}} \tag{3}$$

$$\eta_{gas-SOFC,\ AC\ gross} = \frac{P_{ACgross}}{\dot{m}_{biom} \cdot LHV_{biom}} \tag{4}$$

$$\eta_{gas-SOFC,CHP\ gross} = \frac{P_{ACgross} + \dot{Q}_{SOFC}}{(\dot{m}_{biom} \cdot LHV_{biom})} \tag{5}$$

Regarding the analysis performed in TRNSYS, one of the parameters calculated is the saving of non-renewable (primary) energy, for the three systems (RES1, RES2, RES3) described in Table 1, in comparison to the existing reference system (NRES). For the reference system, the primary energy consumption is the sum of three components: the consumption of electricity for the coverage of electric loads (E_{EL}), the electric energy needed to drive the VCC (E_{VCC}) for the coverage of cooling loads and the consumption of methane for the coverage of heating loads (E_{CH4}). The electric energy needed to drive the auxiliaries (mainly the pumps and the fans of the

Please cite this article in press as: Palomba V, et al., Tri-generation for industrial applications: Development of a simulation model for a gasification-SOFC based system, International Journal of Hydrogen Energy (2017), http://dx.doi.org/10.1016/j.ijhydene.2017.06.206

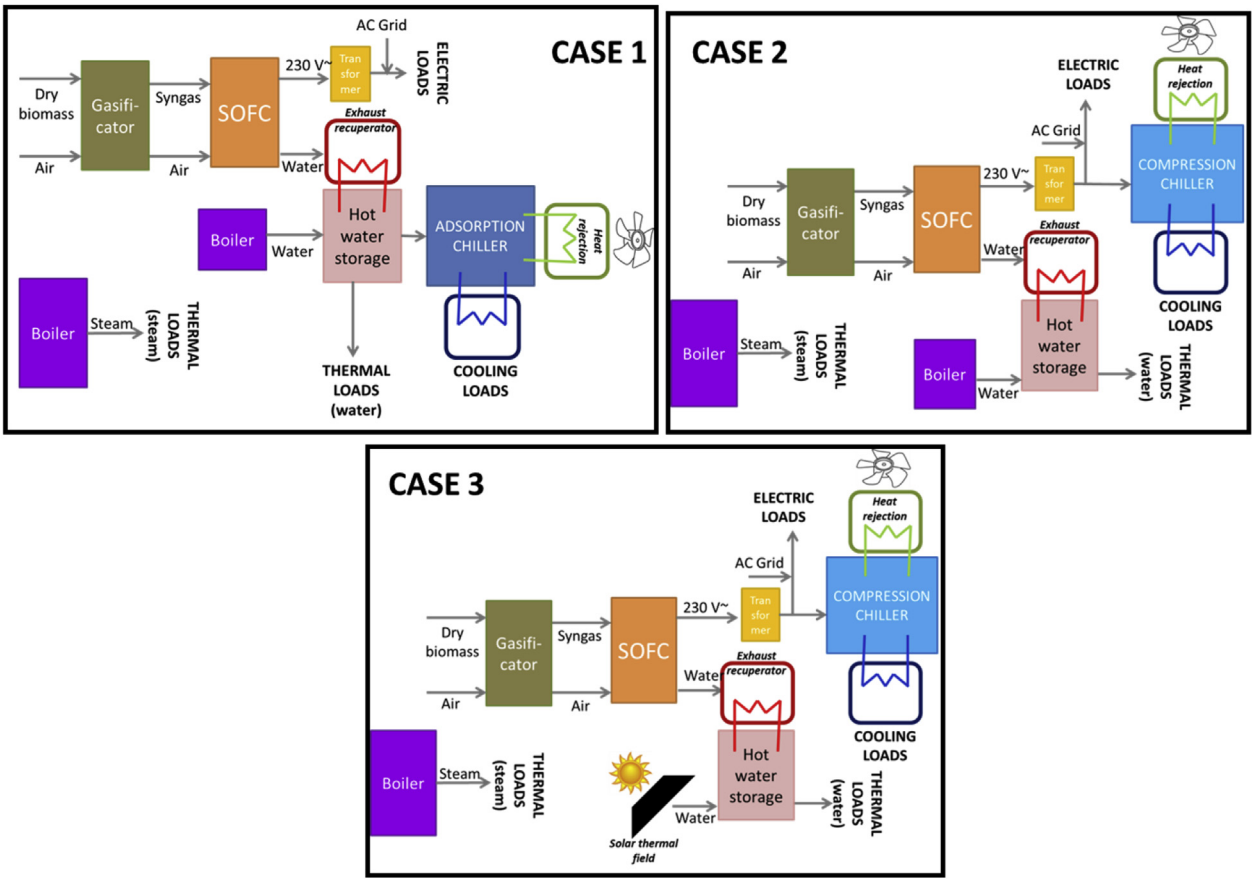

Fig. 2 – Schematic layout of the three simulated scenarios.

recooler) has been included in the calculation as well (E_{aux}). However, since a rigorous energy analysis requires that the compared systems produce the exact same amount of energy, an extra term has been considered ($E_{el,ex}$): it considers that the reference system uses non-renewable energy to produce the same amount of electric energy that is sold to the grid by the renewable systems. Consequently, the primary energy consumed by the reference system is calculated as:

$$PE_{NRES} = \frac{E_{EL} + E_{VCC} + E_{aux}}{\eta_{pd,elec}} + \frac{E_{CH4}}{\eta_{pd,\ CH4}} + \frac{E_{EL,\ ex}}{\eta_{pd,\ elec}} \quad (6)$$

where η_{pd} are the production and dispatch efficiencies detailed in Table 2. The energy needed to drive the vapour compression chiller is a function of the cooling loads (E_{CL}) and its energy efficiency ratio (EER), while the energy due to methane consumption is a function of the heating load and the combustion efficiency of the boiler:

$$E_{VCC} = \frac{E_{CL}}{EER_{VCC}} \quad (7)$$

$$E_{CH4} = \frac{E_{HL}}{\eta_{comb}} \quad (8)$$

For the trigeneration systems, the primary energy consumption is due to the methane consumed by the boiler for steam production and the integrations, in terms of hot water and electricity, of the back-up systems when the energy produced by the fuel cell is not enough to meet the instantaneous demand. It can be expressed as:

$$PE_{RES,\ i} = \frac{E_{elec,\ back-up}}{\eta_{pd,\ elec}} + \frac{E_{CH4,back-up}}{\eta_{pd,\ CH4}} \quad i = 1, 2, 3 \quad (9)$$

The production and dispatch efficiencies for electricity and methane production have been extracted from literature [39]. In Table 2 the parameters used in the above mentioned equations are reported.

In order to directly compare the three systems, and to define if a higher efficiency can be obtained by combined production of heating, cooling and electricity over the separated one, the overall efficiency of the system has been defined as:

$$\eta_{system} = \frac{E_{EL} + E_{HL} + E_{CL}}{E_{biomass} + E_{CH4} + E_{elec,back-up}} \quad (10)$$

It represents the ratio between the useful effect produced by the system (calculated over 1 year operation), in terms of electric loads (EL), heating loads (HL), cooling loads (CL) and the energy supplied to the system, from the biomass, the methane and the electric grid.

Finally, the avoided CO_2 emissions have been calculated as:

$$\Delta CO_{2,\ i} = CO_{2,\ NRES} - CO_{2,\ RESi} = \frac{PE_{NRES} - PE_{RES,\ i}}{\eta_{CO_2}} \quad (11)$$

Please cite this article in press as: Palomba V, et al., Tri-generation for industrial applications: Development of a simulation model for a gasification-SOFC based system, International Journal of Hydrogen Energy (2017), http://dx.doi.org/10.1016/j.ijhydene.2017.06.206

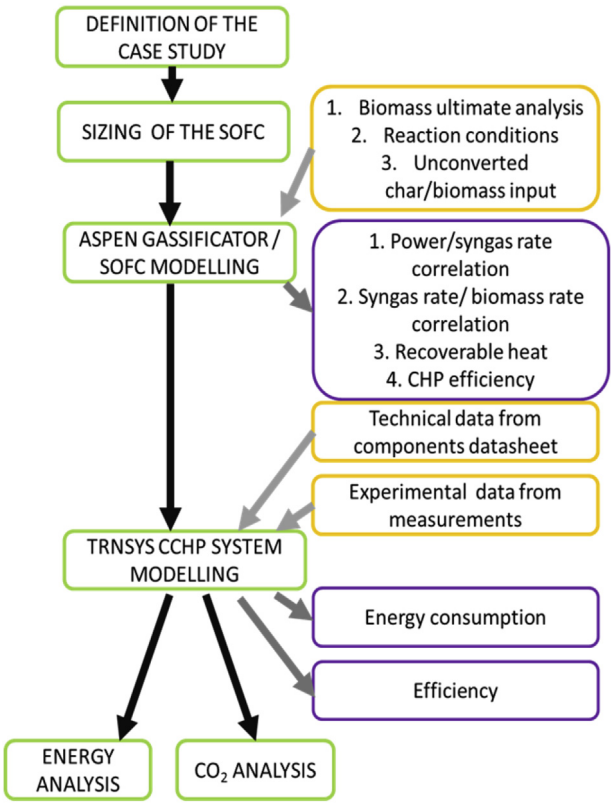

Fig. 3 – Methodology.

The CO_2 emission factor for Italy (η_{CO_2}) has been taken from Ref. [40] and it is equal to 0.39 t/MWh.

Gasification and SOFC models

The downdraft reactor was chosen because it proved to be a reliable and simple solution for small-medium scale commercial solutions [41], which is also able to produce a syngas with very low tar concentration, thus reducing the efforts for gas cleaning. In this work, air was considered as gasification agent, as this is the most common configuration in commercial scale downdraft gasifiers. Furthermore, detailed information has been found for the model development and scale-up of system [42]. The downdraft gasification reactor as well as the SOFC unit were simulated, by means of Aspen Plus simulation software, in order to analyse and predict performances of both syngas production and utilization units. In particular, a steady state simulation model was developed because the start-up and shut-down periods can be neglected if compared to the annual operating hours. With regard to the downdraft reactor, the model aims at simulating the experimental results obtained by Machin et al. [42], which provided substantial experimental details for the model development. The proposed reactor model (orange box in Fig. A. 1, Appendix A) is based on the minimization of the Gibbs free energy. The biomass cannot be described by a conventional chemical component, so it is modelled by a so-called "non-conventional component", whose main feature is the ultimate analysis, as reported in Table 3 for the pine wood [42], which was used as biomass source in this study.

After the validation of the gasification model, whose results are shown in paragraph 6, it was integrated with the model of the solid oxide fuel cell, connecting the produced syngas into the SOFC. The fuel cell model was realised according to the typical SOFC simulation model [25,43,44]. The electric performance were calculated by the well-established equations for the voltage loss, as described in Refs. [43–46]. Doherty [43] described and listed in detail the cell geometry and properties used as input for the voltage calculation, as well as the details for the calculation of each diffusion coefficient. In this work, the same cell properties have been used in order to replicate the SOFC model. The gasification-SOFC model description, as well as the equations used for the syngas flow rate determination, are described in Appendix A.

Table 2 – Parameters used for primary energy calculations.

Parameter	Value
EER_{VCC}	4.0
η_{comb}	0.85
$\eta_{pd,el}$	0.44
$\eta_{pd,CH4}$	0.88

TRNSYS model

TRNSYS environment has been chosen for the simulation of the whole CCHP system, since it includes all the main components for this kind of energy system. In the implementation of the model, for the solar section and the adsorption chillers, previous works by the authors have been used as basis [38,47]. A list of the type used for each component is reported in Table 4, while a detailed description of the types used and their equations is presented in Appendix B.

Among the components used, the adsorption chiller is modelled using a performance map measured at CNR-ITAE while the electric chiller model uses a performance map given by the producer. The other components models, particularly the solar collectors, hot water storage and recooler, have already been validated by the authors, as reported in Ref. [48].

In addition to the main components for power production, other auxiliaries have been inserted in the TRNSYS model of the system. More specifically, they consist of:

- Variable speed pumps, one for each circuit;
- A heat exchanger for the connection of the diathermic oil boiler producing steam to the loads;
- Controllers.

Experimental activity on the adsorption chiller

The model of the adsorption chiller is based on the performance of a commercial chiller measured experimentally at CNR-ITAE. A detailed description of the testing bench used for

Please cite this article in press as: Palomba V, et al., Tri-generation for industrial applications: Development of a simulation model for a gasification-SOFC based system, International Journal of Hydrogen Energy (2017), http://dx.doi.org/10.1016/j.ijhydene.2017.06.206

Table 3 – Ultimate analysis and heating value of pine wood, used as gasification model input.

Ultimate analysis (%wt db)						
C	H	N	O[a]	Ash	Moisture	LHV
%wt db	%wt db	%wt db	%wt db	%wt db	%wt	MJ/kg
48.18	5.71	0.15	43.89	2.07	9.0	17.7

[a] By difference.

such measurements is given in Ref. [49], while a picture of the system is shown in Fig. 4. The main components of the testing bench are:

- a gas heater (1), that is connected to a hot water storage (2) which provides heat for the desorption of the thermally driven chiller at temperatures of 65 °C–90 °C;
- a 63 kW chiller (not shown in the picture) that is connected to a MT/LT storage (3) used to simulate both the condensation circuit at temperatures of 20 °C–45 °C and the user circuit (evaporator circuit) at 10 °C–20 °C. The temperature in both circuit is regulated by means of 3-way valves and PID thermoregulators.
- Variable speed pumps (4) installed in all circuits, as to adjust the flow rate according to the nominal conditions of the chiller.

The measurements on the commercial unit were realised under the following boundary conditions:

- Hot water inlet temperature of 65 °C, 75 °C, 85 °C, 90 °C;
- Heat rejection temperature of 20 °C, 22 °C, 25 °C, 28 °C, 31 °C, 33 °C, 35 °C, 40 °C
- Chilled water temperature of 15 °C and 18 °C.

An example of temperature and power trends recorded during the experimental campaign are shown in Fig. 5 and Fig. 6. In Fig. 5, it is possible to detect the typical operation of an adsorption chiller, characterized by a cyclical trends: at the beginning of each phase, there is a peak in the medium temperature circuit, due to the high condensation rate. Similarly, the temperature of the chilled water outlet is lower at the beginning of each cycle and progressively raises until a new cycle is started. What is clear from the recorded data is that the controlling algorithm of the chiller causes a small variation in the duration of each cycle. The power follows the behaviour of the temperatures, and therefore a peak is visible at the beginning of each cycle, that, for the test shown, reaches 10 kW for the chilled water circuit and 20 kW for the high temperature circuit, representing the amount of heat to be supplied to the system.

During the experimental benchmarking, the thermal Coefficient of Performance of the chiller, its cooling capacity and the electrical consumption were monitored, in order to be able to draw the map of performance used as in input in the model.

Table 4 – TRNSYS type used in the simulation.

Component	TRNSYS type
Heat exchanger	5
Variable speed pump	3 b
Load profile input	14 h
Load to temperature (water)	682
Load to temperature (steam)	605
Adsorption chiller	909
Water-water electric chiller	666
Recooler	511
Hot water storage	60 d
Solar collectors	71
Weather data	15–2

Results and discussion

Validation of downdraft gasification model

In Table 5 the simulation results of the gasification model and the experimental ones reported by Machin et al. [42] are compared. During the stand-alone model validation, the same biomass flow rate (2.5 kg/h) of the experimental tests has been used. It should be noticed that in this simulation model the tar formation has been neglected, as well as the syngas cleaning section. This comes from the very low tar concentration in the produced syngas, as evidenced in Ref. [42]. Furthermore, the analysis of the syngas cleaning section is not object of this paper. The validation results showed a good agreement with the experimental data. The main differences were detected in the syngas heating values, that are higher in the experimental case, due to the absence of methane in the syngas from the simulation model. This difference is equal to 0.12 MJ/Nm^3 and it is caused by the difficulty of the simulation model to form methane at the process conditions (T > 800 °C). Indeed, the simulated syngas composition was obtained with a thermodynamic approach based on the Gibbs free energy minimization.

Gasification – SOFC models integration and system performance

After the stand-alone model validation, the gasifier and the SOFC models have been integrated and the system was scaled up to the plant size (840 kW DC). In the scaled-up system model, the same streams ratios reported in Table 5 have been used. It should be highlighted that, when the two models were integrated, the water in the outlet syngas stream was not condensed. Indeed, it was kept in vapour phase in the syngas stream in order to avoid carbon deposition and favoring the reforming and gas shift reactions in the pre-reformer block of the SOFC. Therefore, the additional water stream entering the SOFC was set to zero for this case study. It follows that in the gasification-SOFC integrated model the composition of wet syngas entering the SOFC is (in %vol.): 10.5% H_2, 13.6% CO, 11.8% CO_2, 51.3% N_2 and 12.8% H_2O. The effect of current density on DC power density, voltage and AC efficiency, using the specified wet syngas composition, are reported in Fig. 7. These curves, that were determined as reported in Appendix A, are used to choose the optimal fuel cell operating conditions. It is trivial to understand that the fuel cell should operate at high efficiency in order to minimize the operating

Please cite this article in press as: Palomba V, et al., Tri-generation for industrial applications: Development of a simulation model for a gasification-SOFC based system, International Journal of Hydrogen Energy (2017), http://dx.doi.org/10.1016/j.ijhydene.2017.06.206

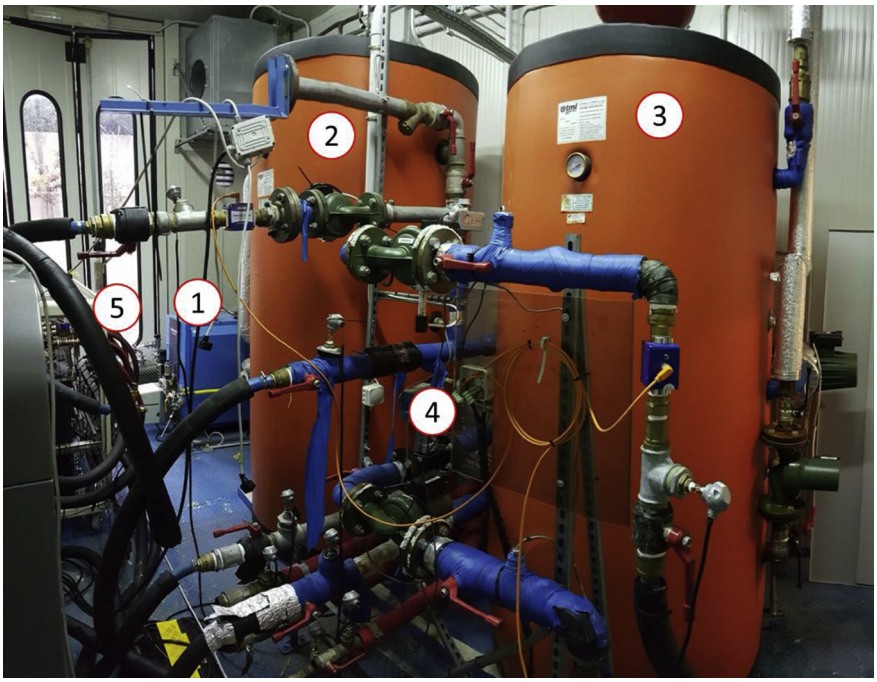

Fig. 4 – The testing bench for the characterization of thermally driven chillers at ITAE; 1-Heater, 2-Hot storage, 3-MT/LT storage, 4-Hydraulic connections, 5-Chiller under testing.

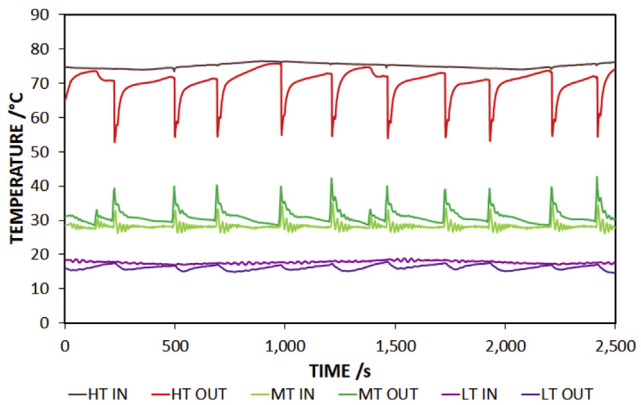

Fig. 5 – Temperature trends during a typical measurement at CNR-ITAE.

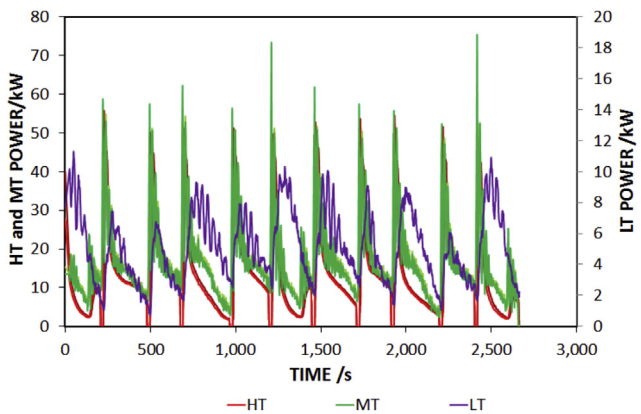

Fig. 6 – Power trends during a measurement.

costs. Instead, to reduce the capital costs, the SOFC should operate at high power density in order to reduce the number of cells. It follows that there must be a trade-off between operating costs (efficiency and voltage) and capital costs (power density). In this work, the SOFC model was operated at 200 mA/cm^2, which is a value in the practical operating range of the tubular solid oxide fuel cell examined in this study [25,43,44].

Table 6 shows the most relevant results of the gasificator-SOFC integrated simulation model. Cold gas efficiency is 55%, in accordance with the performances of the considered downdraft reactor fed with pine wood [42]. The low value of cold gas efficiency may be addressed to the unconverted char that leads to an inefficiency in the gasification process. The biomass input is 700 kg/h of dry biomass, corresponding to 3440 kW, that is required to feed the 840 kW DC SOFC. Its AC gross and net efficiencies are 44% and 36%, respectively, operating at 200 mA/cm^2 and 744 mV. These operating conditions and efficiencies are consistent with realistic ones [25,43]. The gap between the SOFC's gross and net electrical efficiencies is due to the power consumption of syngas and air compressors, accounting for about 161 kW. This leads to a lack of 20% of AC power (the ratio between compressor consumption and gross AC power), while in the case study of Doherty it is about 13% [43]. This difference is due to the high concentration of nitrogen in the syngas obtained in this case study (51.3% vol. wet basis), which dilutes the syngas, leading to a higher syngas flow rate needed to feed the SOFC. This implies higher compression work. Conversely, the well-known Güssing dual fluidized bed air-steam gasification allows the production of an almost nitrogen-free syngas (1% vol. dry basis) [43]. The low cold gas efficiency has a negative impact on the plant gross electrical efficiency (23%), as

Please cite this article in press as: Palomba V, et al., Tri-generation for industrial applications: Development of a simulation model for a gasification-SOFC based system, International Journal of Hydrogen Energy (2017), http://dx.doi.org/10.1016/j.ijhydene.2017.06.206

Table 5 – Experimental and simulated data of the downdraft gasification unit.

Parameter	Unit	Experimental [29]	Model	Difference between experimental and models
Air/biom (20°C)	(kg/kg_{ar})	2.58	2.56	1.0%
(Char + ash)/biom	(kg/kg_{ar})	0.051	0.050	1.0%
Dry syngas/biom	(kg/kg_{ar})	3.27	3.21	1.0%
Water out/Biom	(kg/kg_{ar})	0.281	0.297	5.4%
Dry syngas composition				
H_2	(% vol.)	12.1	12.0	1.0%
CO	(% vol.)	16.0	15.7	1.9%
CO_2	(% vol.)	11.4	13.3	14.2%
CH_4	(% vol.)	0.2	–	–
N_2	(% vol.)	59.4	58.9	1.0%
LHV	(MJ/Nm^3)	3.40	3.28	3.6%

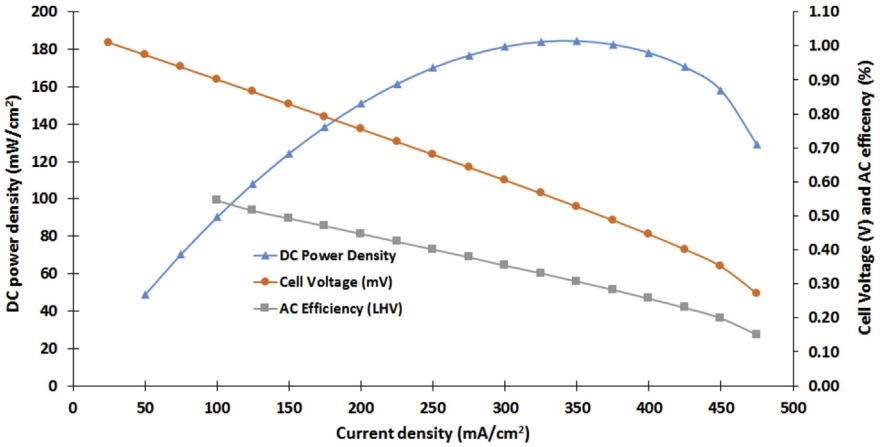

Fig. 7 – Polarization curve, power density and cell performance as function of current density.

reported in Table 6. This value is lower than other biomass gasification-SOFC systems analysed in literature [25,27,43]. It follows that even the plant CHP efficiency results to be lower than expected [25,43]. The above results indicate how the gasification process efficiency and the specific gasification technology may affect the system efficiency. In fact, if a typical cold gas efficiency of about 75% would be reached, the plant gross electrical efficiency may achieve values of about 34%, that is comparable with efficiency obtained by Doherty et al. [25,43]. Furthermore, when the nitrogen content in the producer gas, the net efficiency enhances due to the reduction of the required power for syngas compression. This goal may be achieved using an air-steam gasification, instead of an air gasification, and using a dual bed reactor to separate the combustion flue gas (nitrogen rich) from the syngas produced during steam gasification reactions [25,41,43].

Table 6 – Main results of the Gasification-SOFC system.

Parameter	Unit	Value
Gasification unit		
Biomass input	kW	3440
Cold gas efficiency (LHV basis)	–	55%
SOFC unit		
Current density	mA/cm^2	200
Cell voltage (mV)	mV	744
Net DC power	kW	840
Gross AC power	kW	790
Net AC power	kW	629
SOFC AC gross efficiency	–	44%
SOFC AC net efficiency	–	36%
Integrated gasification – SOFC plant		
Gasificator-SOFC gross electrical efficiency	–	23%
Max. recoverable heat from the SOFC	kW	1185
Gasificator-SOFC gross CHP efficiency (LHV basis)	–	56%

Integration of the models

In literature, different approaches have been used for the simulation of fuel cells in TRNSYS, as the integration with MATLAB models [30], or the utilization of a performance map [35,50]. In the present work, the characteristic curves of the SOFC system, showing the syngas flow rate and thermal power output as a function of the SOFC AC power, have been derived and are shown in Fig. 8(a–c). As visible, the simulation points from ASPEN can be fitted with straight lines, whose equations are shown in the graphs. The linear trends are due to the fact that the CHP system is made up of several stacks of 120 kW DC, each unit working at 100% of its capacity. The reduction of the electrical power output was achieved by reducing the number of operating SOFCs stacks. A macro has then been created in TRNSYS, including these equations. It also includes the correlation that is used to simulate the gasification unit, showing the

Please cite this article in press as: Palomba V, et al., Tri-generation for industrial applications: Development of a simulation model for a gasification-SOFC based system, International Journal of Hydrogen Energy (2017), http://dx.doi.org/10.1016/j.ijhydene.2017.06.206

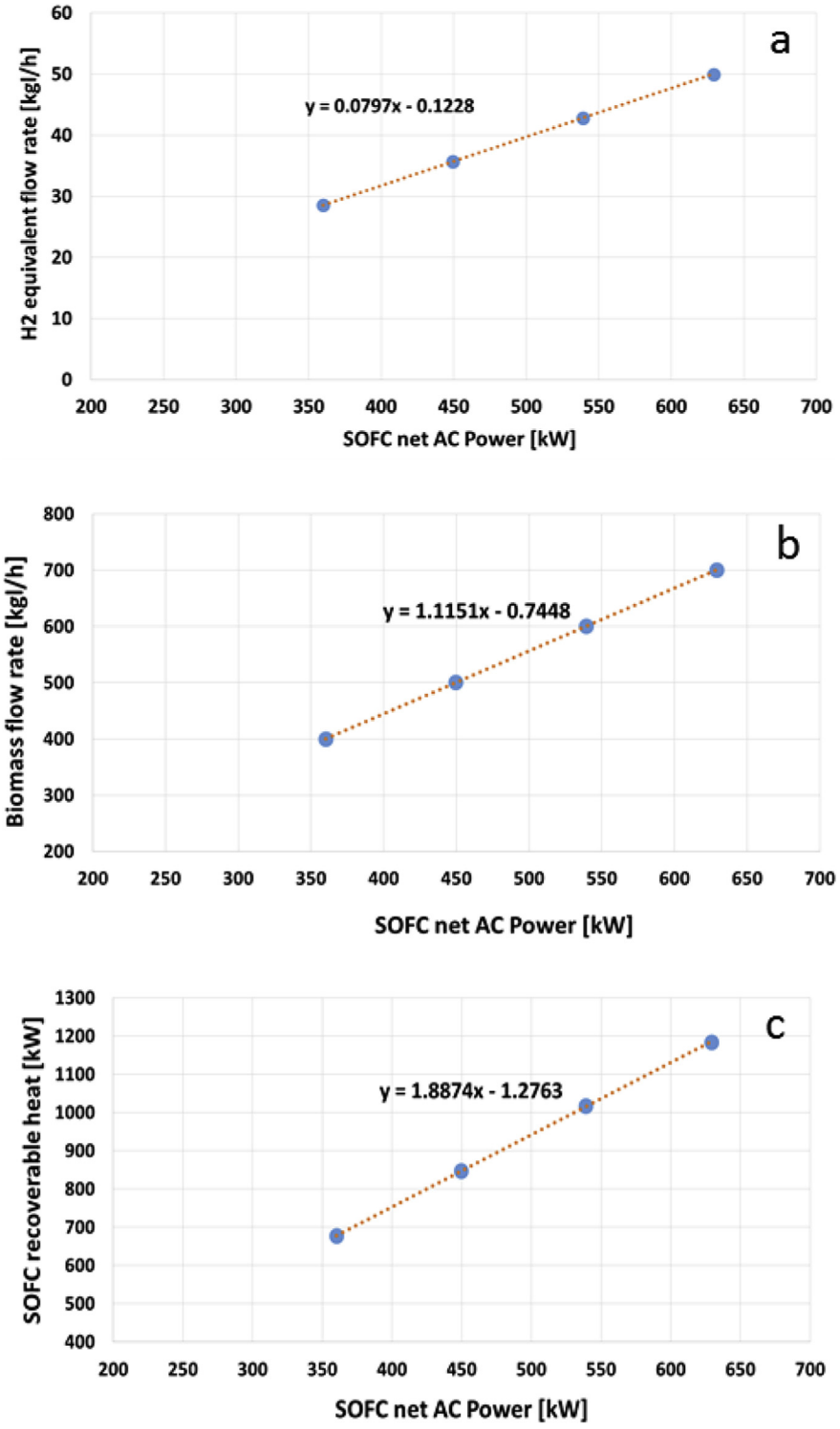

Fig. 8 – Relationship between SOFC net AC Power and hydrogen equivalent mass flow rate (a), biomass mass flow rate (b) and SOFC recoverable heat (c).

amount of biomass needed to drive the gasification-SOFC system (Fig. 8b). This relationship can be used to determine the annual biomass rate, that is the main energy input of the system. The TRNSYS is structured so that it uses the desired electrical power from the SOFC as input and, by means of the equations shown in Fig. 8(a–c), gives as output the recoverable heat and the biomass flow rate.

Energy analysis

One of the main reasons to replace a traditional system with a CCHP one, is the higher overall efficiency in power generation. Since the analysed layouts involve different sources and several energy conversion components, Sankey diagram has

Please cite this article in press as: Palomba V, et al., Tri-generation for industrial applications: Development of a simulation model for a gasification-SOFC based system, International Journal of Hydrogen Energy (2017), http://dx.doi.org/10.1016/j.ijhydene.2017.06.206

been used to identify all the energy streams and the utilization of energy. Energy flows for the three cases examined are represented in Fig. 9, Fig. 10 and Fig. 11 on annual basis. In all scenarios, the highest energy contribution is due to the biomass supplied to the gasificator-SOFC system. The energy due to methane is mainly used to cover the steam demands. It is higher in case 1, because in this layout the heat from the SOFC is mainly used to drive the adsorption chiller. However, in this case, the electric energy supplied by the grid is lower, because in the other scenarios, a higher electric energy share is needed to drive the electric chiller. In case 3, the heat from the fossil-fuelled boiler is only needed for steam production, while the other heating loads are completely met by the SOFC and solar thermal collectors. The heat losses through the environment have been calculated as well: they consist in the heat of condensation of the adsorption or VCC chiller, that must be rejected through the dry recooler: the highest value is those of case 1, when the adsorption chiller is used.

The overall efficiency of the system has been calculated as well, according to Eq. (10). For case 1, it is equal to 34%, while for case 2 is 36% and for case 3 is 37%. The efficiency for a separate production of heat, cold and electricity is instead equal to 27%, about a quarter less than the efficiency for the combined production. Indeed, as previously explained, the overall efficiency of the system is negatively affected by the low efficiency of the CHP section, thus indicating that an even further improvement could be achieved by choosing a different type of gasificator. Considering the comparison between the three layouts, the higher efficiency of case 2 and case 3 is mainly due to the heating demand. Indeed, differently from what found in literature for residential applications, where the heating loads are comparatively small [38,47], in this specific application, with a relevant heating load, the utilization of heat from SOFC to drive the adsorption chiller represents a disadvantageous choice. On the contrary, since the electric loads are significantly smaller, excess electricity to drive the vapour compression chiller leads to a better utilization of the energy produced. The difference between case 2 and case 3 is very small. It is actually true that, for case 3, the integration of boilers for the production of hot water is

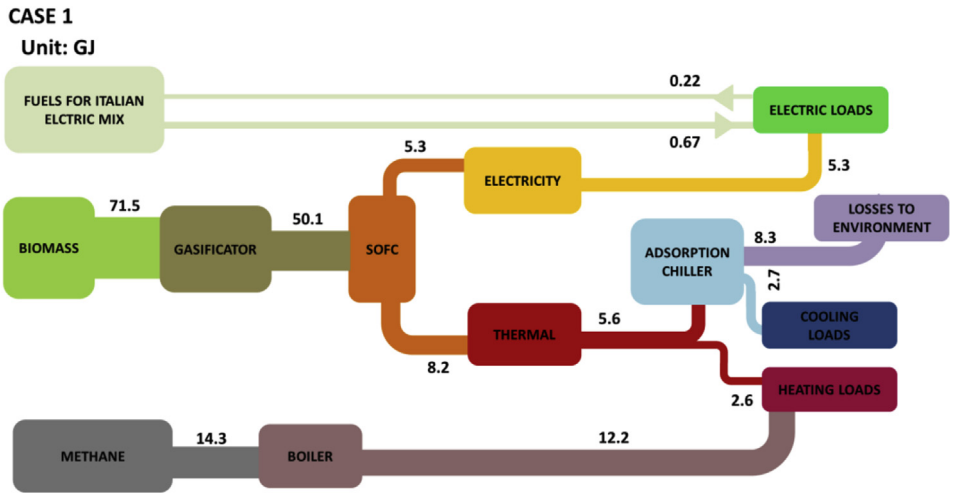

Fig. 9 – Energy flow for case 1.

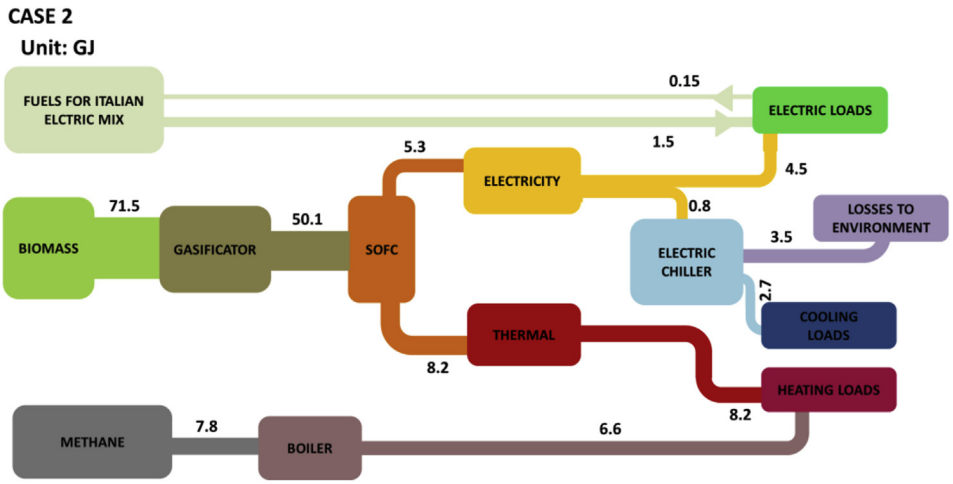

Fig. 10 – Energy flow for case 2.

Please cite this article in press as: Palomba V, et al., Tri-generation for industrial applications: Development of a simulation model for a gasification-SOFC based system, International Journal of Hydrogen Energy (2017), http://dx.doi.org/10.1016/j.ijhydene.2017.06.206

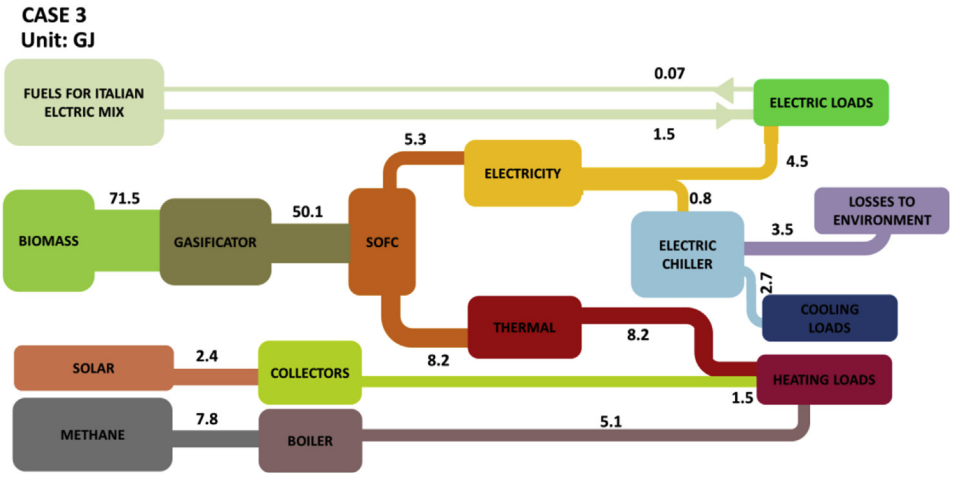

Fig. 11 – Energy flow for case 3.

completely removed, but at the expense of a more complicated and expensive system layout since it includes solar collectors. Moreover, a boiler for the production of steam is still present, therefore the system cannot run on 100% renewables.

From TRNSYS model, the annual amount of biomass needed has been calculated to be 5500 t/y.

Fig. 12 shows the non-renewable primary energy savings for the three systems, on monthly basis and for the simulation of the entire year. The differences among the three cases are around 5%, with the system from case 3 performing better, since energy from solar collectors replaces part of the energy needed for the covering of heating loads. Case 1 and case 2 allow for savings of non-renewable primary energy of 48%, while case 3 allows primary energy savings of 52%, corresponding to 15 GWh for the entire year.

The results of the energy analysis indicate that, even though the overall efficiency of the system is almost the same for case 2 and 3, the installation of solar thermal collectors increases the primary energy savings, that, as shown below, corresponds to lower CO_2 emissions. All the proposed solutions perform better than the reference system and permit reducing the energy from traditional sources.

Environmental analysis

Fig. 13 shows the emissions avoided in the three cases. The trends match those of the primary energy savings, with a more consistent benefit for case 3 and a similar behaviour for case 1 and case 2. The avoided emissions are around half of those for the traditional system, and are equal to 5000 t/y, which is therefore a significant reduction.

Comparison with a gasification-I.C.E system

The results obtained in the study here presented have been compared to the ones obtained by the authors in Ref. [51], where the same application was considered using an internal combustion engine instead of a SOFC to satisfy electricity demand and the heating loads, while cooling loads were

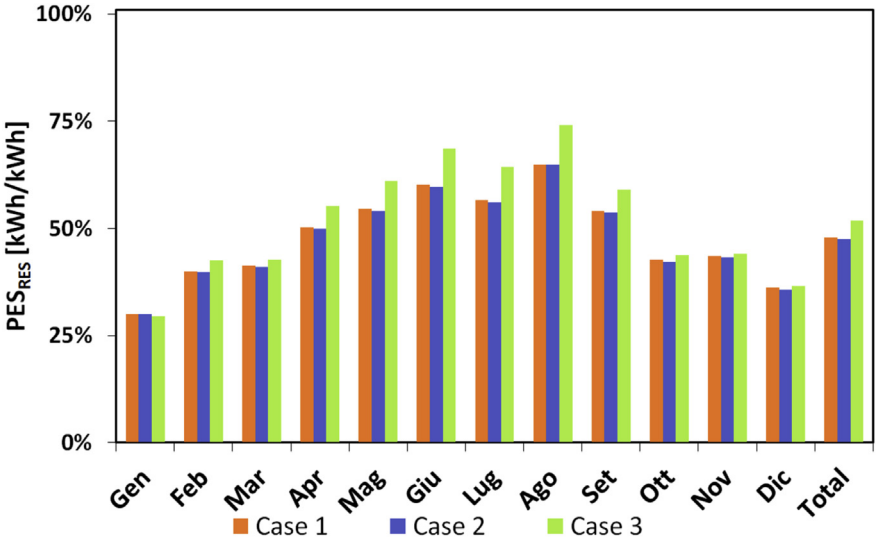

Fig. 12 – Primary energy savings in the various scenarios.

Please cite this article in press as: Palomba V, et al., Tri-generation for industrial applications: Development of a simulation model for a gasification-SOFC based system, International Journal of Hydrogen Energy (2017), http://dx.doi.org/10.1016/j.ijhydene.2017.06.206

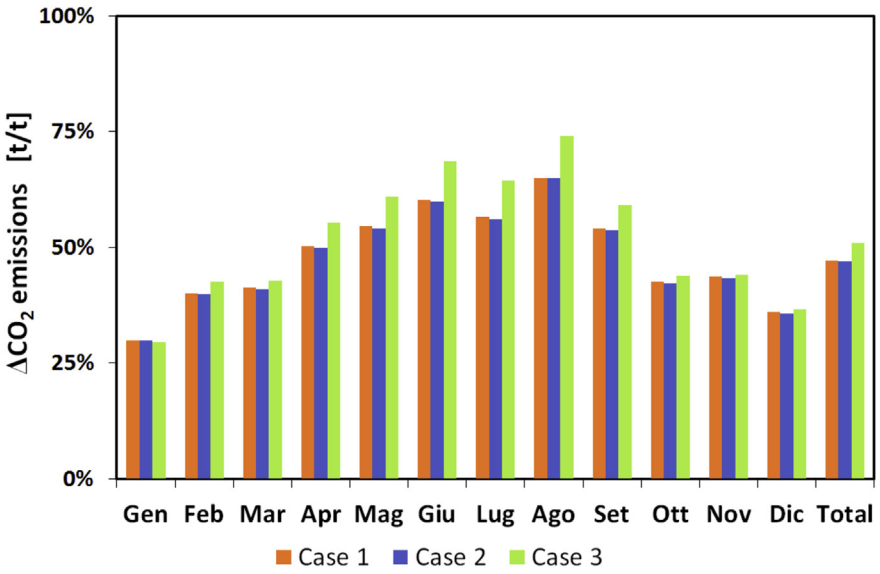

Fig. 13 – Avoided carbon dioxide emissions in the various scenarios.

fulfilled with electric chillers. The results obtained, in terms of primary energy savings and avoided CO_2 emissions are similar to those found for the case of scenario 2: the primary energy needed to drive the system was 49% of that for the reference system. However, the overall efficiency of the system, calculated according to Eq. (10) for the gasification-I.C.E. based case is 29%, which is lower than the system here proposed, thus highlighting the more efficient production obtainable with a SOFC system.

Conclusions

The potential of integrating a gasification-SOFC CHP system in an existing manufacturing production process has been evaluated by means of simulation models. The biomass used as feedstock was the residue of pine wood processing that is produced by the wood processing industry that has been selected for this work. The actual heat and power generation system (reference system) installed in the considered industrial site has been compared with three different alternatives for heating and cooling production. Each of the proposed alternatives had a biomass gasification-SOFC system for the base load power generation. The gasification-SOFC simulation model has been developed by ASPEN Plus simulation software, while TRSNSYS was used for the integration of the SOFC into the whole trigeneration system. All the models were based on validated components. The results of the gasification-SOFC model showed that plant gross electrical and CHP efficiencies are 23% and 56%, respectively. The low efficiency can be addressed to the low cold gas efficiency of the analysed downdraft air gasification system that was found to be 55%. The SOFC AC gross efficiency is about 44%, which is comparable with literature data. It follows that the weakest link of the proposed gasification-SOFC system is the gasification step and that improving the biomass conversion process can positively reflect on the electrical and CHP efficiencies of the power unit. The results of the gasification-SOFC model have been used to integrate it in a TRNSYS model. The integration was obtained by adding the equations describing the relationships between the SOFC AC net output and the SOFC thermal output varying the biomass input. Using this tool, energetic and environmental analysis have been performed, showing a saving of about 50% of primary energy and an avoided CO_2 emission of about 5000 t/y compared to the existing reference system. The overall efficiency of the system is 34%, 36% and 37% for the three cases respectively, whereas the efficiency of the existing system for separate energy production is 27%. Finally, the amount of biomass needed to run the system has been estimated in 5500 t/y.

Appendix A. Gasification – SOFC model

The gasification-SOFC model is shown in Fig. A. 1. The stream named "BIOMASS" describes the wet biomass input, which first meet a RYield block (H2OYIELD) that separates the intrinsic moisture of biomass from the non-conventional substream, according to the proximate analysis, while a separation block (H2OSEP) separates the moisture from the dry biomass (DRYBIOM) stream, in order to direct the water into the gasification reactor. The dried biomass is then decomposed in its elementary compounds (BIOMELEM stream), according to the ultimate analysis, in the "BIOMDEC" block (an RYIELD block), in which ash is modelled with silicon. The yields of the biomass elements at the output of the RYIELD blocks are calculated from the biomass ultimate analysis. Unconverted char and ash are separated from the main stream according to the ash + char yields obtained experimentally [42]. The elements that constitutes the dry-ash-free biomass are directed in the part of the reactor in which the combustion reactions take place ("COMB" block). The temperature of this block is set at 900 °C [42] and it is fed by hot air, which is heated up to 200 °C thanks to the hot syngas. The air flow rate is set in order to keep the experimental air/biomass ratio reported in Ref. [25]. The products of the incomplete combustion feed the "GASIFIC" block, in which the

Please cite this article in press as: Palomba V, et al., Tri-generation for industrial applications: Development of a simulation model for a gasification-SOFC based system, International Journal of Hydrogen Energy (2017), http://dx.doi.org/10.1016/j.ijhydene.2017.06.206

gasification reactions take place. This block is kept at 830 °C [42] and it is also fed by the moisture released in the drying zone, which reacts with unburned char and products of the partial combustion. The solution with moisture reacting in the gasification zone gave good matching results with experimental data. An alternative solution could be to direct the moisture out from the reactor without participating to the reactions, but it did not give satisfactory results. Both combustion and gasification zones have been represented by the ideal Gibbs reactors. The additional heat exchanger after the air heater was added for a syngas temperature adjustment.

The syngas produced in the gasification unit is directed to the SOFC and it is compressed by means of the "COMP-1" block up to 3 bar. Then the syngas is preheated by the recirculated gas from the anode outlet. A pre-reformer is also present in order to conduct further reforming and gas-shift reactions, before entering the anode. The unreacted syngas is then directed to a post-combustion reactor, which allows to increase the fuel cell heat output. The cell voltage calculation has been carried out according to the following equation [43–46]:

$$V = V_N - V_{Ohm} - V_a - V_C \quad \text{(A.1)}$$

where V_N is the Nernst voltage, and V_{Ohm}, V_a and V_c are the ohmic, activation and concentration voltage losses. The last equation allows to determine the polarization curves when applied at different current density values. The terms of the above equations, related to voltage losses, were calculated according to equations available in literature for these tubular SOFC systems [43–46]. Doherty et al. listed in detail the cell geometrical parameters and materials properties used for tubular SOFC developed by Siemens [43]. The authors described and validated the replicated SOFC model in a previous work [45]. The SOFC simulation model outputs are (i) the cell voltage (0.744 V at 200 mA/cm^2), (ii) the required hydrogen molar flow (kmol/h) and (iii) the syngas molar flow (kmol/h). The last two have been calculated according to the following equations:

$$n_{H_2,\,in} = \frac{I \cdot 3600}{2FU_f \times 1000} \quad \text{(A.2)}$$

$$n_{Fuel_{in}} = \frac{n_{H_2,in}}{x_{H_2} + x_{CO} + 4 \cdot x_{CH4}} \quad \text{(A.3)}$$

where $n_{H_2,in}$ and $nFuel_{in}$ are expressed in kmol/h, while F and x are the Faraday constant (C/mol) and the molar fraction of gaseous components, respectively. In this work, the fuel cell model was operated with a current density of 200 mA/cm^2 and considering a specific active area of 0.0834 m^2/cell. The syngas molar flow ($nFuel_{in}$) was the input for a "design specification" unit, available in the simulation software, which varies the biomass flow rate until the specified syngas flow rate is reached. The correct air/biomass ratio was secured placing a calculation block before the air heater (AIRH block). Hence, the air flow rate was determine by the following equation introduced in the calculation air calculation unit:

$$AIR = BIOMASS \cdot 2.56 \quad \text{(A.4)}$$

where AIR and BIOMASS are the mass flow rates of air and biomass, respectively.

The heat recovered from the SOFC unit was obtained from the "RECHEAT" stream in Fig. A. 1.

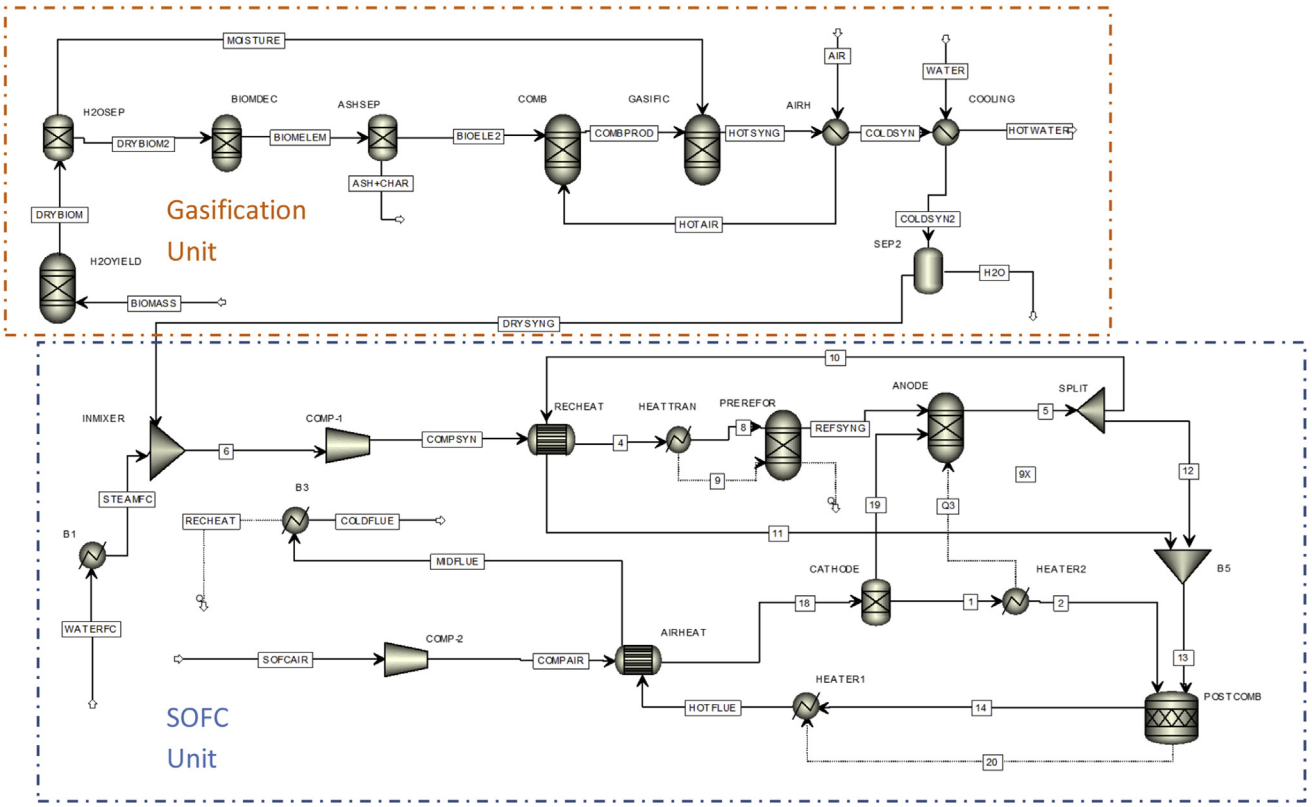

Fig. A 1 – Simulation model of the gasification-SOFC system.

Please cite this article in press as: Palomba V, et al., Tri-generation for industrial applications: Development of a simulation model for a gasification-SOFC based system, International Journal of Hydrogen Energy (2017), http://dx.doi.org/10.1016/j.ijhydene.2017.06.206

Appendix B. TRNSYS model

In the present appendix, more detailed information on the TRNSYS model will be given, including the types used, the equations and correlations that have been implemented and the parameters selected. For the equations that are not indicated, the detailed description or solver routine can be found in Ref. [52]. The time step chosen is 15 min.

Heat exchangers

All the heat exchangers have been modelled using TRNSYS type 5, where the UA value is provided by the user and the effectiveness is calculated for each configuration [52]. In the present case, a cross flow mode with non-mixing streams has been considered. The UA values for the water recuperator from SOFC has been considered equal to 500 W/K, while the distribution of cold to the cooling loads has been considered through a connection to a heat exchanger with UA of 1000 W/K.

Variable speed pump

Pumps have been modelled by means of Type3b as variable speed pumps, that can provide any outlet mass flow rate between zero and a rated value. The mass flow rate provided by the pump varies linearly with control signal. Efficiency of the pump can be modelled by using a polynomial expression, but in the present case only the first order coefficient has been employed. A summary of the pumps, the nominal flow rates and efficiency is given in Table B. 1.

Table B 1 – Features of the pumps for the modelled system.

Pump	Nominal flow rate [kg/h]	Power consumption at nominal [W]
Hot water outlet from SOFC	2000	300
Hot water outlet from water recuperator	1000	300
Back-up boiler for water	500	500
Boiler for steam	3000	800
Solar loop (case 3)	1000	600
Hot water adsorption chiller (case 1)	19,000	1000
Heat rejection adsorption chiller (case 1)	25,000	1000
Chilled water adsorption chiller (case 1)	17,000	1000
Heat rejection electric chiller (cases 2 and 3)	25,000	1000
Chilled water electric chiller (cases 2 and 3)	17,000	1000

Load to temperature

Since all the loads were available as a profile of instant power needed for each hour, the interaction with the other components of the system was realised using two types that allow imposing the heating or cooling load on a fluid stream.

For water flows, type 682 was used. In this type, the fluid flow rate, heat capacity and the temperature in one point of the fluid stream are specified as inlet, and the solver calculates the outlet temperature as:

$$T_{out} = T_{in} \pm \frac{\dot{Q}}{\dot{m} c_p} \tag{B.1}$$

The sign (+ or -) in the previous equation, depends on whether the load is defined as heating or cooling.

The same principle is used for the steam loads, simulated by means of type 605, which takes into account also the enthalpy for the steam flow.

Evacuated tube solar collectors

In the layout from case 3, a 1000 m^2 solar field has been considered, made up of evacuated tube collectors. The performance of a solar collector can be expressed as a function of its average temperature as follows [53]:

$$\frac{Q}{A} = G\left(a_0 - a_1\frac{T_m - T_{amb}}{G} - a_2\frac{(T_m - T_{amb})^2}{G}\right) \tag{B.2}$$

Where Q is the power output from solar collectors, A is the surface of the collector, G is the intensity of solar radiation, T_m is the collector average temperature and T_a is the ambient temperature. The parameters in the equation are summarised in the table below.

Table B 2 – Parameters used in Eq. B.2.

Parameter	Unit	Value
a0	–	0.586
a1	W/m^2K	1.485
a2	W/m^2K^2	0.002

Moreover, incident angle modifiers have been used to describe the ratio of the efficiency measured at actual admitted irradiance to vertical admitted irradiance.

Table B 3 – IAM for the solar collectors modelled.

Angle	10	20	30	40	50	60	70
$K\theta lon$	1.00	1.00	0.99	0.98	0.97	0.94	0.88
$K\theta tran$	1.35	1.17	1.25	1.20	1.22	1.15	0.83
Incident angle modifier K_θ (40.2°/40.2°)	1.186						

Storage tank

The modelled storage tank is a stratified storage with heat loss coefficient of 0.95 W/°C. An internal heat exchanger has been considered for the connection of solar thermal circuit in case 3 and the connection of back-up boiler in case 1. For calculation on the thermal storage system, TRNSYS routines divides the tank into nodes and performs an energy balance on each of them, as described in Ref. [52]. The volume of the storage tank volume is 40 m^3 for cases 1 and 2 and 50 m^3 for case 3, chosen in order to be able to store all the energy recovered from SOFC.

Please cite this article in press as: Palomba V, et al., Tri-generation for industrial applications: Development of a simulation model for a gasification-SOFC based system, International Journal of Hydrogen Energy (2017), http://dx.doi.org/10.1016/j.ijhydene.2017.06.206

Re-cooler

The dry fluid cooler used is based on TRNSYS type 511, in which the design conditions (flow rates and temperature) are inserted as parameters, together with the desired outlet temperature. The model, first uses design data to determine the UA of the heat exchanger at design conditions, then corrects design UA according to instant inlet conditions and finally calculates the air flow rate required in order for the dry fluid cooler to deliver the specified outlet liquid temperature. A complete description of the mathematical model can be found in Ref. [52], instead the features of the simulated recooler, based on the specifications of a commercial unit, are reported in Table B. 4.

Table B 4 – Parameters for the simulated recooler.

Parameter	Unit	Value
Design inlet fluid temperature	°C	30.6
Design outlet fluid temperature	°C	25
Design fluid flow rate	kg/h	25,000
Design air flow rate	kg/h	400,000
Rated fan power	kW	5.4

Chillers

Both chillers (adsorption and electric) have been simulated using a performance-map based approach. Such a performance map includes cooling capacity and COP of the chiller as a function of temperature levels and, in the case of the electric chiller, part load effect. The solver then reads the inlet conditions and interpolates the data according to the ones supplied by the user (without extrapolating them, in order to improve the reliability of the model). In both cases, commercial units have been considered:

- for the electric chiller, a 320 kW unit using R410A, with rated COP of 4.5. The data to be employed in type 666 are taken from the datasheet supplied by the producer.
- for the adsorption chiller, data measured at ITAE on a silica gel/water commercial unit with rated power of 10 kW have been used. As pointed out before, the rated power needed for the cooling unit is 320 kW, while the one of the unit measured at ITAE is only 10 kW. Therefore the scaling of the chiller is necessary. Indeed, TRNSYS type 909 is intrinsically built to fulfil such a need: for each experimental point, the cooling capacity and COP are inserted as a fraction of the nominal values. Consequently, when scaling the system, it is sufficient to define the scaled nominal power and COP and the solver's routine will take that into account. In particular, as a result of the experiment, a nominal capacity of 10.2 kW was defined, with a nominal COP of 0.6.

REFERENCES

[1] Davis J, Caldeira K, Matthews HD. Future CO_2 emissions and climate change from existing energy infrastructure. Science 2010;329(5997):1330–3.
[2] Raupach MR, Marland G, Ciais P, Le Quéré C, Canadell JG, Klepper G, et al. Global and regional drivers of accelerating CO_2 emissions. Proc Natl Acad Sci U S A 2007;104:10288–93. http://dx.doi.org/10.1073/pnas.0700609104.
[3] Joselin Herbert GM, Unni Krishnan A. Quantifying environmental performance of biomass energy. Renew Sustain Energy Rev 2016;59:292–308. http://dx.doi.org/10.1016/j.rser.2015.12.254.
[4] Perea-Moreno A-J, Miguel-Ángel PM, Hernandez-Escobedo Q, Manzano-Agugliaro F. Towards forest sustainability in Mediterranean countries using biomass as fuel for heating. J Clean Prod 2017. http://dx.doi.org/10.1016/j.jclepro.2017.04.091.
[5] Basu P. Biomass gasification, pyrolysis and torrefaction: practical design and theory. Academic Press; 2013.
[6] Patel M, Zhang X, Kumar A. Techno-economic and life cycle assessment on lignocellulosic biomass thermochemical conversion technologies: a review. Renew Sustain Energy Rev 2016;53:1486–99. http://dx.doi.org/10.1016/j.rser.2015.09.070.
[7] Yaman S. Pyrolysis of biomass to produce fuels and chemical feedstocks. Energy Convers Manag 2004;45:651–71. http://dx.doi.org/10.1016/S0196-8904(03)00177-8.
[8] Gądek W, Mlonka-Mędrala M, Prestipino M, Evangelopoulos P, Kalisz S, Yang W. Gasification and pyrolysis of different biomasses in lab scale system: a comparative study. E3S Web Conf 2016;10. http://dx.doi.org/10.1051/e3sconf/20161000024. 24.
[9] Voloshin RA, Rodionova MV, Zharmukhamedov SK, Nejat Veziroglu T, Allakhverdiev SI. Review: biofuel production from plant and algal biomass. Int J Hydrogen Energy 2016;41:17257–73. http://dx.doi.org/10.1016/j.ijhydene.2016.07.084.
[10] Martínez JD, Mahkamov K, Andrade RV, Silva Lora EE. Syngas production in downdraft biomass gasifiers and its application using internal combustion engines. Renew Energy 2012;38:1–9. http://dx.doi.org/10.1016/j.renene.2011.07.035.
[11] Sansaniwal SK, Pal K, Rosen MA, Tyagi SK. Recent advances in the development of biomass gasification technology: a comprehensive review. Renew Sustain Energy Rev 2017;72:363–84. http://dx.doi.org/10.1016/j.rser.2017.01.038.
[12] Sorgenfrei M, Tsatsaronis G. Detailed exergetic evaluation of heavy-duty gas turbine systems running on natural gas and syngas. Energy Convers Manag 2016;107:43–51. http://dx.doi.org/10.1016/j.enconman.2015.03.111.
[13] Brusca S, Galvagno A, Lanzafame R, Garrano AMC, Messina M. Performance analysis of biofuel fed gas turbine. Energy Procedia 2015;81:493–504. http://dx.doi.org/10.1016/j.egypro.2015.12.123.
[14] Schicktanz MD, Wapler J, Henning H-M. Primary energy and economic analysis of combined heating, cooling and power systems. Energy 2011;36:575–85. http://dx.doi.org/10.1016/j.energy.2010.10.002.
[15] Cannistraro G, Cannistraro M, Cannistraro A, Galvagno A, Trovato G. Technical and economic evaluations about the integration of co-trigeneration systems in the dairy industry. Int J Heat Technol 2016;34:332–6. http://dx.doi.org/10.18280/ijht.34S220.
[16] Pagliarini G, Corradi C, Rainieri S. Hospital CHCP system optimization assisted by TRNSYS building energy simulation tool. Appl Therm Eng 2012;44:150–8. http://dx.doi.org/10.1016/j.applthermaleng.2012.04.001.
[17] Liu M, Aravind PV, Woudstra T, Cobas VRM, Verkooijen AHM. Development of an integrated gasifier–solid oxide fuel cell test system: a detailed system study. J Power Sources 2011;196:7277–89. http://dx.doi.org/10.1016/j.jpowsour.2011.02.065.
[18] Chiodo V, Zafarana G, Maisano S, Freni S, Galvagno A, Urbani F. Molten carbonate fuel cell system fed with biofuels

Please cite this article in press as: Palomba V, et al., Tri-generation for industrial applications: Development of a simulation model for a gasification-SOFC based system, International Journal of Hydrogen Energy (2017), http://dx.doi.org/10.1016/j.ijhydene.2017.06.206

for electricity production. Int J Hydrogen Energy 2016;41:18815–21. http://dx.doi.org/10.1016/j.ijhydene.2016.05.119.
[19] Urbani F, Freni S, Galvagno A, Chiodo V. MCFC integrated system in a biodiesel production process. J Power Sources 2011;196:2691–8. http://dx.doi.org/10.1016/j.jpowsour.2010.11.024.
[20] Gucciardi E, Chiodo V, Freni S, Cavallaro S, Galvagno A, Bart JCJ. Ethanol and dimethyl ether steam reforming on Rh/Al_2O_3 catalysts for high-temperature fuel-cell feeds. React Kinet Mech Catal 2011;104:75–87. http://dx.doi.org/10.1007/s11144-011-0335-y.
[21] Panopoulos KD, Fryda LE, Karl J, Poulou S, Kakaras E. High temperature solid oxide fuel cell integrated with novel allothermal biomass gasification: part I: modelling and feasibility study. J Power Sources 2006;159:570–85. http://dx.doi.org/10.1016/j.jpowsour.2005.12.024.
[22] Singhal S. Advances in solid oxide fuel cell technology. Solid State Ionics 2000;135:305–13. http://dx.doi.org/10.1016/S0167-2738(00)00452-5.
[23] Santarelli M, Briesemeister L, Gandiglio M, Herrmann S, Kuczynski P, Kupecki J, et al. Carbon recovery and re-utilization (CRR) from the exhaust of a solid oxide fuel cell (SOFC): analysis through a proof-of-concept. J CO_2 Util 2017;18:206–21. http://dx.doi.org/10.1016/j.jcou.2017.01.014.
[24] Ozcan H. Performance evaluation of an SOFC based trigeneration system using various gaseous fuels from biomass gasification. Int J Hydrogen Energy 2015;40:7798–807. http://dx.doi.org/10.1016/j.ijhydene.2014.11.109.
[25] Doherty W, Reynolds A, Kennedy D. Process simulation of biomass gasification integrated with a solid oxide fuel cell stack. J Power Sources 2015;277:292–303. http://dx.doi.org/10.1016/j.jpowsour.2014.11.125.
[26] Vialetto G, Noro M, Rokni M. Innovative household systems based on solid oxide fuel cells for the Mediterranean climate. Int J Hydrogen Energy 2015;40:14378–91. http://dx.doi.org/10.1016/j.ijhydene.2015.03.085.
[27] Wongchanapai S, Iwai H, Saito M, Yoshida H. Performance evaluation of an integrated small-scale SOFC-biomass gasification power generation system. J Power Sources 2012;216:314–22. http://dx.doi.org/10.1016/j.jpowsour.2012.05.098.
[28] Kupecki J, Skrzypkiewicz M, Wierzbicki M, Stepien M. Experimental and numerical analysis of a serial connection of two SOFC stacks in a micro-CHP system fed by biogas. Int J Hydrogen Energy 2017;42:3487–97. http://dx.doi.org/10.1016/j.ijhydene.2016.07.222.
[29] Al Moussawi H, Fardoun F, Louahlia-Gualous H. Review of tri-generation technologies: design evaluation, optimization, decision-making, and selection approach. Energy Convers Manag 2016;120:157–96. http://dx.doi.org/10.1016/j.enconman.2016.04.085.
[30] Calise F. Design of a hybrid polygeneration system with solar collectors and a solid oxide fuel cell: dynamic simulation and economic assessment. Int J Hydrogen Energy 2011;36:6128–50. http://dx.doi.org/10.1016/j.ijhydene.2011.02.057.
[31] Calise F, Ferruzzi G, Vanoli L. Transient simulation of polygeneration systems based on PEM fuel cells and solar heating and cooling technologies. Energy 2012;41:18–30. http://dx.doi.org/10.1016/j.energy.2011.05.027.
[32] Frazzica A, Briguglio N, Sapienza A, Freni A, Brunaccini G, Antonucci V, et al. Analysis of different heat pumping technologies integrating small scale solid oxide fuel cell system for more efficient building heating systems. Int J Hydrogen Energy 2015;40:14746–56. http://dx.doi.org/10.1016/j.ijhydene.2015.08.003.
[33] Sibilio S, Rosato A, Ciampi G, Scorpio M, Akisawa A. Building-integrated trigeneration system: energy, environmental and economic dynamic performance assessment for Italian residential applications. Renew Sustain Energy Rev 2017;68:920–33. http://dx.doi.org/10.1016/j.rser.2016.02.011.
[34] Fong KF, Lee CK. System analysis and appraisal of SOFC-primed micro cogeneration for residential application in subtropical region. Energy Build 2016;128:819–26. http://dx.doi.org/10.1016/j.enbuild.2016.07.060.
[35] Kazempoor P, Dorer V, Weber A. Modelling and evaluation of building integrated SOFC systems. Int J Hydrogen Energy 2011;36:13241–9. http://dx.doi.org/10.1016/j.ijhydene.2010.11.003.
[36] Jradi M, Riffat S. Tri-generation systems: energy policies, prime movers, cooling technologies, configurations and operation strategies. Renew Sustain Energy Rev 2014;32:396–415. http://dx.doi.org/10.1016/j.rser.2014.01.039.
[37] Heidenreich S, Foscolo PU. New concepts in biomass gasification. Prog Energy Combust Sci 2015;46:72–95. http://dx.doi.org/10.1016/j.pecs.2014.06.002.
[38] Vasta S, Palomba V, Frazzica A, Di Bella G, Freni A. Techno-economic analysis of solar cooling systems for residential buildings in Italy. J Sol Energy Eng Trans ASME 2016;138. http://dx.doi.org/10.1115/1.4032772.
[39] Taylor P, Lavagne D'Ortique O, Trudeau N, Francoueur M. Energy efficiency indicators for public electricity production from frossil fuels. n.d.
[40] Statistics I. CO2 emissions from fuel combustion. 2015.
[41] Jong W de, Ommen JR van. Biomass as a sustainable energy source for the future: fundamentals of conversion processes. n.d.
[42] Machin EB, Pedroso DT, Proenza N, Silveira JL, Conti L, Braga LB, et al. Tar reduction in downdraft biomass gasifier using a primary method. Renew Energy 2015;78:478–83. http://dx.doi.org/10.1016/j.renene.2014.12.069.
[43] Doherty W, Reynolds A, Kennedy D. Computer simulation of a biomass gasification-solid oxide fuel cell power system using Aspen Plus. Energy 2010;35:4545–55. http://dx.doi.org/10.1016/j.energy.2010.04.051.
[44] Zhang W, Croiset E, Douglas PL, Fowler MW, Entchev E. Simulation of a tubular solid oxide fuel cell stack using AspenPlusTM unit operation models. Energy Convers Manag 2005;46:181–96. http://dx.doi.org/10.1016/j.enconman.2004.03.002.
[45] Galvagno A, Prestipino M, Zafarana G, Chiodo V. Analysis of an integrated agro-waste gasification and 120kW SOFC CHP system: modeling and experimental investigation. Energy Procedia 2016;101:528–35. http://dx.doi.org/10.1016/j.egypro.2016.11.067.
[46] Bove R, Ubertini S. Modeling solid oxide fuel cell operation: approaches, techniques and results. J Power Sources 2006;159:543–59. http://dx.doi.org/10.1016/j.jpowsour.2005.11.045.
[47] Vasta S, Palomba V, Frazzica A, Costa F, Freni A. Dynamic simulation and performance analysis of solar cooling systems in Italy. Energy Procedia 2015;81. http://dx.doi.org/10.1016/j.egypro.2015.12.146.
[48] Palomba V, Vasta S, Freni A, Pan Q, Wang R, Zhai X. Increasing the share of renewables through adsorption solar cooling: a validated case study. Renew Energy 2016. http://dx.doi.org/10.1016/j.renene.2016.12.016.
[49] Sapienza A, Gullì G, Calabrese L, Palomba V, Frazzica A, Brancato V, et al. An innovative adsorptive chiller prototype based on 3 hybrid coated/granular adsorbers. Appl Energy 2016;179. http://dx.doi.org/10.1016/j.apenergy.2016.07.056.
[50] Dorer V, Weber A. Energy and CO2 emissions performance assessment of residential micro-cogeneration systems with dynamic whole-building simulation programs. Energy Convers Manag 2009;50:648–57. http://dx.doi.org/10.1016/j.enconman.2008.10.012.

Please cite this article in press as: Palomba V, et al., Tri-generation for industrial applications: Development of a simulation model for a gasification-SOFC based system, International Journal of Hydrogen Energy (2017), http://dx.doi.org/10.1016/j.ijhydene.2017.06.206

[51] Prestipino M, Palomba V, Vasta S, Freni A, Galvagno A. A simulation tool to evaluate the feasibility of a gasification-I.C.E. System to produce heat and power for industrial applications. Energy Procedia 2016;101:1256–63. http://dx.doi.org/10.1016/j.egypro.2016.11.141.

[52] Solar Energy Laboratory U of W. TRNSYS 17 documentation. n.d.

[53] Duffie JA, Beckman WA. Solar engineering of thermal processes. Wiley; 2013.

Please cite this article in press as: Palomba V, et al., Tri-generation for industrial applications: Development of a simulation model for a gasification-SOFC based system, International Journal of Hydrogen Energy (2017), http://dx.doi.org/10.1016/j.ijhydene.2017.06.206